Ice-sheet sounding at X, L and UHF bands from high altitude by vertical SAR imaging

Hubert Cantalloube

▶ **To cite this version:**

Hubert Cantalloube. Ice-sheet sounding at X, L and UHF bands from high altitude by vertical SAR imaging. EUSAR 2021, Mar 2021, VIRTUEL, Germany. hal-03243440

HAL Id: hal-03243440
https://hal.science/hal-03243440

Submitted on 31 May 2021

HAL is a multi-disciplinary open access archive for the deposit and dissemination of scientific research documents, whether they are published or not. The documents may come from teaching and research institutions in France or abroad, or from public or private research centers.

L'archive ouverte pluridisciplinaire **HAL**, est destinée au dépôt et à la diffusion de documents scientifiques de niveau recherche, publiés ou non, émanant des établissements d'enseignement et de recherche français ou étrangers, des laboratoires publics ou privés.

Ice-sheet sounding at X, L and UHF bands from high altitude by vertical SAR imaging.

Hubert M.J. Cantalloube[a]
[a]ONERA Université Paris Saclay, F-91123 Palaiseau, France

Abstract

Though generally used for side-looking "push-broom" imaging, the synthetic aperture radar principle can, as well, be applied to nadir looking vertical plane imaging. Vertical SAR has proven useful e.g. for high altitude altimetric accurate navigation resetting. During the 2017 ONERA campaign in Greenland, this imaging mode was investigated for assessment of snow/ice radar penetration in the ice-sheet. At UHF-band, it provides a clear image of subsurface ice density discontinuities up to a depth of few tens of meters, comparable to images obtained from ground penetrating radar (GPR) operated directly at the surface. The possibility of acquiring such images from a safer distance at a much higher velocity should increase the throughput of future glaciology campaigns on polar ice-sheets.

1 Introduction

1.1 Context

Following the loss of an engine fan assembly by a jet-liner above the Greenland ice-sheet [1], ONERA had been approached for localising fragments that escaped optical detection from early explorations of the accident area and were critical for the accident cause investigation. Due to the regular snow falls, fragments are progressively buried under a thicker and thicker snow/ice layer. ONERA carried out a SAR survey at X, L and UHF bands of the area 6 months after the accident with is Sethi airborne radar system (**Figure 1**). After intensive processing, this survey eventually yielded three detections of critical heavy fragments. 21 month after the accident, digging at the first detection location allowed GEUS glaciologists to recover a significant fan hub fragment. Upon investigation on the recovered fragment, the engine manufacturer issued a preventive maintenance mitigation for the accident cause.

Figure 1 ONERA SAR system (SETHI) as operated in Greenland. Pod under the left wing contains the UHF antenna looking to the left at 45°incidence. Pod under the right wing contains L-band antenna looking to the left (though orientable in flight from horizon to horizon) and X-band antenna looking to the right (orientable in flight from horizon to nadir)

1.2 Motivation for vertical SAR

1.2.1 for the engine fragment search

With approximately 1.5 m snow fall between the accident and the SAR acquisitions, the fragments depth was expected to be in the 1 to 3 m range. Hence the different snow/ice penetration capabilities at the different radar bands, as well as the icesheet backscatter levels are extremely relevant to the target detectability. Though penetration can be indirectly derived from interferometric techniques (e.g. by measuring the altitude bias of the InSAR-derived DTM with respect to surface measurement[2] or by the coherency variation with incidence angle[3]) direct nadir observation, when possible, provides a penetration assessment that is not altered by trajectory (baseline) nor delay drift (radar parameters drift) errors between the two interferometric acquisitions.

Furthermore, the accuracy of trajectory (nominaly 20 cm vertical) and of the internal delays measurements (typically below 1 ns) means that the ice sheet surface elevation at nadir can be derived with an absolute accuracy of ± 30 cm. This allows to register the DTM which, due to the lack of tiepoint on solid earth within a few hundreds of kilometers, may be altered by a significant bias. Precise altitude of two points at the surface in our operation area had been measured by a glaciologists expedition prior to our SAR survey, but an independent measure along some 16 two km long lines yielded a DTM debiasing critical to our survey success.

1.2.2 other scientific motivations

Ice sounding is generally done using GPR typically in the 100 to 200 MHz band directly from the surface. It has been demonstrated from an aircraft at low altitude and even from

orbit (on the icesheets of planet Mars), but without synthetic aperture, the resolution along-track is limited by the antenna footprint.
Since the interesting features for glaciology are the layer density discontinuities, which are close to horizontal in a glacier accumulation zone such as our search area, we expected them to appear as strong near specular echoes on vertical SAR images.
Comparison of conventional (side-looking) SAR images and vertical SAR sounding within its footprint is also useful to understand the subsurface features that appear at longer wavelength (deeper penetration) on (side-looking) SAR images.

2 vertical SAR acquisitions

Though dedicated acquisitions with antenna pointed to the nadir is possible with our SAR system (**Figure 2**), nadir sounding images in Greenland were obtained with antenna side-lobes during conventional side-looking acquisitions.

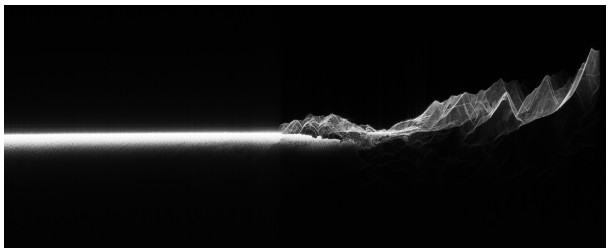

Figure 2 Example of a vertical SAR image acquired with antenna pointed to the nadir. This is the X component of an X+Ku vertical SAR acquisition beginning over the Mediterranean sea, overflying the little coastal town of Banyuls and ending on the Pyreneans heights in South France. It was acquired by the Sethi system in November 15^{th} 2019. Vertical axis is emphasized 4 times for clarity.

Illumination of the nadir with side-lobes of the antenna is avoided when nadir echo may alter the image (e.g. when the altitude to ground falls within a range ambiguity). This is particularly the case for spaceborne SAR systems because propagation loss is huge (typical range is 800 km) and Earth is nearly flat at this "hundreds of km" scale hence the specular nadir reflection if very strong and may saturate the receiver even through low sidelobes. However, in the medium-range wide swath acquisitions of our survey in Greenland, this was not critical neither at X nor L-bands (at UHF band, the mainlobe extends beyond the nadir yielding strong left-right ambiguities at steep incidence).
At both X & L-bands, the sidelobe level at nadir is stronger in vertical polarisation (as antenna pattern is broader along the E field axis). Note however that this "vertical" polarisation from the antenna viewpoint is an horizontal polarisation for the target (ground) because E field is horizontal.
Vertical SAR imaging in the antenna side-lobe was opportunistically demonstrated in 1993 at ONERA (**Figure 3**) while making a C-band polarimetric image of Paris (**Figure 4**). On the top-right image in this figure, the sidelobe image appears in the middle (with the profile of the skyscrapers and the great arch of "La Défense" west of Paris), below it is a dark "antenna pattern node" and at the bottom starts the "conventional" mainlobe side-looking SAR image...

Figure 3 Vertical SAR image of "la Défense" skyscraper ensemble (top) , and a nearly perpendicular optical image (bottom) a photo taken from the Étoile arch rooftop for comparison.

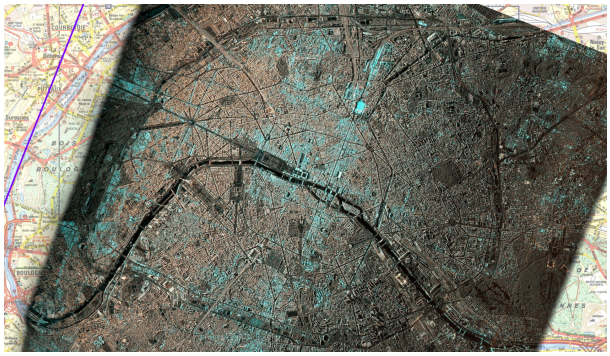

Figure 4 The conventional –side looking– polarimetric SAR image of Paris acquired at C-band in 1993. The aircraft trajectory is the thick purple line at the left (West) of the map. The SAR image of figure 3 is in the vertical plane through that line, and the Étoile arch where picture was taken is the large circle 1 cm above the Eiffel tower.

3 geometry of VSAR acquisition

Native geometry of our SAR processor is conical coordinate from a nominal linear trajectory (conical coordinate system degenerates into the cylindrical coordinate system in the unsquinted "0 Doppler" case). For minimising motion compensation efforts, the nominal trajectory line is choosen as a linear best fit of the actual trajectory (for the processed part of the signal). Since acquisition trajectories are generally at constant altitude (for ATC constraints) the nominal trajectory is pitched down, the actual trajectory starting and ending below it and culminating above it. Note that some airborne SAR system are commonly aiming at linear trajectories that "cut through" the Earth curvature (E.g. the LoraSAR/Carabas system of the Swedish FOI clearly follows that objective).
For steering the synthetic antenna to the nadir, we should

require from the SAR processor a look for a squint angle opposed to the average pitch of the nominal trajectory (due to the Earth curvature, the pitch of the nominal trajectory increases along the line (**Figure 5**)).

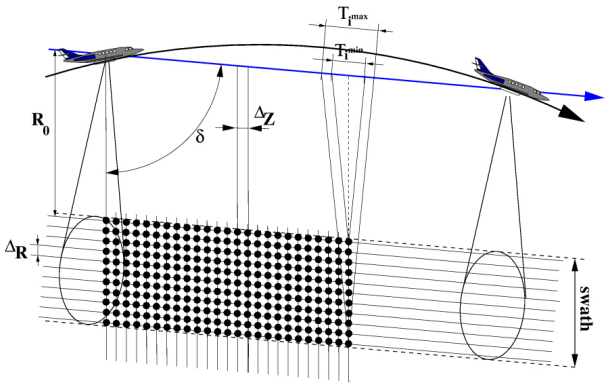

Figure 5 Vertical SAR geometry, with the actual trajectory in fat black line (which aims a constant altitude), the nominal –straight line– trajectory in blue.

For focusing (motion compensating) the image with respect to the vertical plane containing the nominal trajectory, we simply need to ask the processor to "focus without DTM to an arbitrary large negative altitude" (typically -10 000 m). Under these instructions, the SAR processors generates an internal DTM parallel to the Earth Ellipsoid at the corresponding Ellipsoidal altitude. Then, in the preparation for motion compensation, it maps the elevation corresponding to pixels of the final images, and because the corresponding range falls above the DTM surface, it places the focus points in the vertical plane below the nominal trajectory.
Note that for pixels "inside" ground, if echo *is actually* at the surface (hence not below the nominal trajectory) it may be out of focus because of the actual trajectory non-linearities. This is more and more the case as range increases and as surface echo corresponds to a more and more grazing incidence angle. See [4] for details on the motion compensation.

4 Examples of VSAR images of ice-sheet

4.1 X-band VSAR image

Figure 6 illustrate the VSAR images obtained at X-band. On this image, we observe a first (from the top down) echo corresponding to the snow surface, then at a distance of approximately 2.5 m (in vaccuum), there is a much stronger echo. Since 2.5 m in vaccuum corresponds to 1.9 m in a material of index 1.3 (a good starting point for superficial snow), the strong interface most probably correspond to the snow/firn transition (transition between snow fallen during 2017-2018 winter and earlier snow that percolated and refrost the summer melt of 2017).
As seen on the digging for the engine fragment recovery, this transition consists of a 10 cm thick solid ice layer (that appears blue) under which the refrozen snow is denser

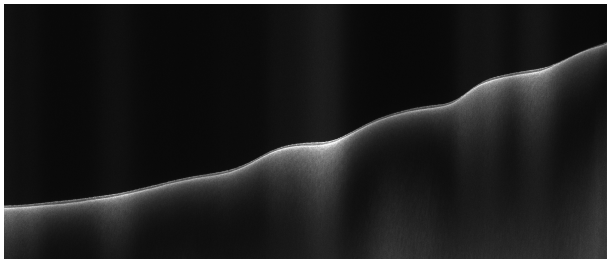

Figure 6 Vertical SAR image of the ice-sheet at X band. Horizontal axis is along track (10 km of acquisition). Vertical axis is altitude (300 m from the bottom to the top). Unlike the convention used for GPR, echoes are white, and black area corresponds to the atmosphere above the snow surface.

(with probably an higher refractive index).

4.2 L-band VSAR image

At L-band, the range resolution is much lower (1 m) than at X-band (20 cm in Figure 6), hence the separation between surface and snow/firn transition echoes is less salient, but the first two summer melts are clearly visible on **Figure 7**. Careful observation shows that further summer melts can be detected up to a vaccum equivalent depth of $\simeq$11.5 m which should correspond to $\simeq$8.8 m real depth.

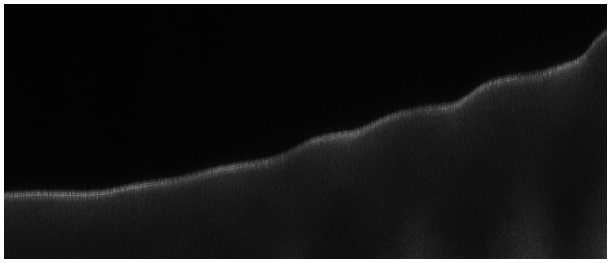

Figure 7 Vertical SAR image of the ice-sheet at L band. Horizontal axis is along track (10 km of acquisition). Vertical axis is altitude (300 m from the bottom to the top). Note that the surface altimetric profile is different than at X-band because acquisition trajectory axis is 200 m South of the X-band acquisition.

4.3 UHF-band VSAR image

At UHF-band, the range resolution is higher (65 cm) than at L-band and the snow/ice penetration is even higher. On the image in **Figure 9** we can observe layer transitions up to a vaccuum-equivalent depth of 38.5 m (closer to 30 m of real depth). This last salient echo would correspond to a summer meltdown circa 1998 (or perhaps to the snow-to-ice transition due to static pressure).
Note also a stronger echo at a vaccuum-equivalent depth of 15 m (closer to 11 m real depth) that should be the thicker ice layer of the great meltdown of 2012 (an exceptional heat wave that melted the Greenland surface up to the highest latitudes).

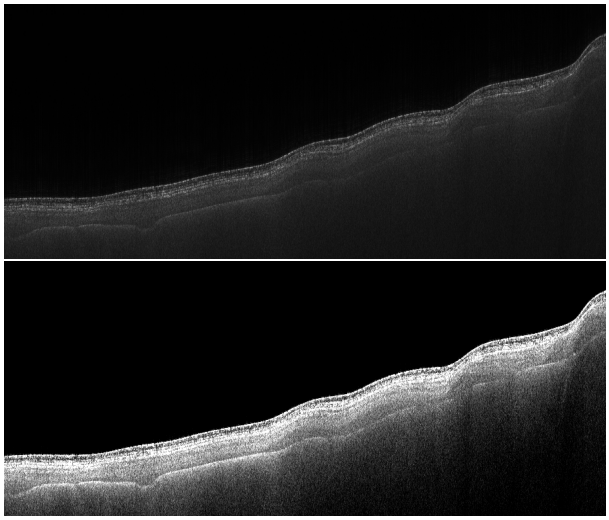

Figure 8 Vertical SAR image of the ice-sheet at UHF band. Horizontal axis is along track (10 km of acquisition). Vertical axis is altitude (300 m from the bottom to the top). Top image is with its native dynamic range, bottom one is with contrast stretched for emphasising the layers transition at deeper altitude.

5 Use of VSAR images to interpret through the ice (conventional) SAR images

Because of the multiple heading acquired for our campaign objective (locate the fan hub fragments), we have conventional SAR images acquisitions of the trace of the VSAR image plane, thus the VSAR images provides "cuts" in the SAR images either along or across track (at X-band) and also in the 45°directions of tracks at L & UHF bands.

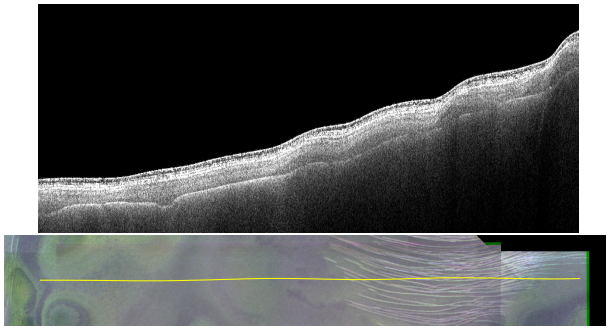

Figure 9 Trajectory overlayed on the UHF composite SAR image (bottom) corresponding to the VSAR image of figure 8 (top). The horizontal polarisation corresponding to the VSAR image is coded to the blue channel of the composite SAR image (green is vertical and red is cross-polarisations).

6 Conclusion

Vertical SAR imaging of the ice-sheet, yields profiles of the buried ice features for a long distance from a safer distance at a much higher velocity than possible from the surface with a GPR. Being also acquired within few hours of conventional SAR images, it may be used to infer the depth of subsurfaces features observed on conventional SAR images that can cover an huge terrain surface compared to direct 2D GPR scan form the surface **Figure 10**.

Figure 10 Example of GPR scan from the surface during the second GEUS polar expedition.

7 Acknowledgements

Thanks to all the ONERA/DEMR EXA & TERE teams under the lead of Pascal Dubois-Fernandez for the SAR campaign preparation and realisation, to the BEA for commissionning ONERA for this accident investigation, Airbus for funding and support, to the Danish GEUS for the valuable ground truth, target setup expedition under the lead of Nanna Karlsson and to the Arctic Command for operational support. ICEsat DEM used for altitude profile comparison were provided by the Polar Geospatial Center under NSF OPP awards 1043681, 1559691 & 1542736

8 Literature

[1] Bureau d'Enquêtes et d'Analyses: Technical report, Accident to the Airbus A380 registered F-HPJE and operated by Air France on 30/09/2017 en route over Greenland, https://www.bea.aero/uploads/tx_elyextendttnews/F-HPJE_TECHNICAL_REPORT.pdf, 2019

[2] Dall, J.: InSAR elevation bias caused by penetration into uniform volumes. IEEE Transactions on Geoscience and Remote Sensing Vol. 45, No. 7, Nov. 2007, pp. 2319-2324

[3] Tishkovets, V.P.: Litvinov, P.V.: Lyubchenko, M.V.: Coherent opposition effects for semi-infinite discrete random medium in the double-scattering approximation, Journal of Quantitative Spectroscopy and Radiative Transfer, Vol. 72, No. 6, 2002, pp.803-811

[4] Cantalloube, Hubert M. J.; Nahum, Carole E.: Airborne SAR-Efficient Signal Processing for Very High Resolution, proc. of the IEEE, Vol. 101, No. 3, Mar. 2013, pp. 784-797